Received: 25 June 2024 | Accepted: 12 August 2024

DOI: 10.1111/jpy.13497

RESEARCH ARTICLE

Photoperiod and temperature interactions drive the latitudinal distribution of *Laminaria hyperborea* (Laminariales, Phaeophyceae) under climate change

Nora Diehl[1,2] | **Philipp Laeseke**[3] | **Inka Bartsch**[2] | **Margot Bligh**[1,4] | **Hagen Buck-Wiese**[4] | **Jan-Hendrik Hehemann**[1,4] | **Sarina Niedzwiedz**[1] | **Niklas Plag**[5,6] | **Ulf Karsten**[5,7] | **Tifeng Shan**[8] | **Kai Bischof**[1]

[1]Faculty of Biology and Chemistry & MARUM, University of Bremen, Bremen, Germany
[2]Alfred Wegener Institute, Helmholtz Centre for Polar and Marine Research, Bremerhaven, Germany
[3]Animal Ecology and Systematics, Justus Liebig University of Giessen, Giessen, Germany
[4]Max Planck Institute for Marine Microbiology, Bremen, Germany
[5]Institute of Biological Sciences, University of Rostock, Rostock, Germany
[6]Julius Kühn-Institute (JKI)—Federal Research Centre for Cultivated Plants, Brunswick, Germany
[7]Interdisciplinary Faculty, Department of Maritime Systems, University of Rostock, Rostock, Germany
[8]Institute of Oceanology, Chinese Academy of Sciences, Qingdao, China

Correspondence
Nora Diehl, Faculty of Biology and Chemistry & MARUM, University of Bremen, D-28359 Bremen, Germany.
Email: ndiehl@uni-bremen.de

Funding information
This study was conducted in the frame of the project FACE-IT (The Future of Arctic Coastal Ecosystems - Identifying Transitions in Fjord Systems and Adjacent Coastal Areas). FACE-IT has received funding from the European Union's Horizon 2020 research and innovation programme under grant agreement, Grant/Award Number: 869154; Deutsche Forschungsgemeinschaft, Grant/Award Number: GR5088/2-1

Editor: C. Camus

Abstract

Due to global rises in temperature, recent studies predict marine species shifting toward higher latitudes. We investigated the impact of interacting abiotic drivers on the distribution potential of the temperate kelp *Laminaria hyperborea*. The ecosystem engineering species is widespread along European coasts but has not yet been observed in the High Arctic, although it can survive several months of low temperatures and darkness. To investigate its ability to extend northward in future, we conducted a long-term multifactorial experiment with sporophytes from Porsangerfjorden, Norway—close to the species' documented northernmost distribution margin. The samples were exposed to three different photoperiods (PolarDay, LongDay, and PolarNight) at 0°C, 5°C, and 10°C for 3 months. Optimum quantum yield of photosynthesis (F_v/F_m), dry weight, pigments, phlorotannins, and storage carbohydrates were monitored. Both physiological and biochemical parameters revealed that *L. hyperborea* was strongly influenced by the different photoperiods and their interaction with temperature, while temperature alone exerted only minor effects. The F_v/F_m data were integrated into a species distribution model to project a possible northward expansion of *L. hyperborea*. The combination of extended day lengths and

---

Abbreviations: 0-LongDay, 0°C and Long Day Treatment; 0-PolarDay, 0°C and Polar Day Treatment; 0-PolarNight, 0°C and Polar Night Treatment; 10-LongDay, 10°C and Long Day Treatment; 10-PolarDay, 10°C and Polar Day Treatment; 10-PolarNight, 10°C and Polar Night Treatment; 5-LongDay, 5°C and Long Day Treatment; 5-PolarDay, 5°C and Polar Day Treatment; 5-PolarNight, 5°C and Polar Night Treatment; Acc, accessory pigments; Chl *a*, chlorophyll *a* (); DPS, de-epoxidation state of the xanthophyll cycle pigments; DW, dry weight; F_v/F_m, maximum quantum yield of photosystem II (in vivo chlorophyll-fluorescence of photosystem II); LD, LongDay; MOPS, 3-Morpholinopropane sulfonic acid; NO_3^-, nitrate; P, photoperiod; PD, PolarDay; PES, Provasoli Enriched Seawater; PN, PolarNight; PO_4^{3-}, phosphate; S, sampling time; SST, sea surface temperature; T, temperature; VAZ, pool of the xanthophyll cycle pigments; w, week; w0, week0; w12, week12; w4, week4; w8, week8.

low temperatures appeared to be the limiting reason for northward spread of *L. hyperborea* until recently. However, with water temperatures reaching 10°C in summer, this kelp will be able to thrive also in the High Arctic. Moreover, no evidence of stress to Arctic winter warming was observed. Consequently, *L. hyperborea* has a high potential for spreading northward with further warming which may significantly affect the structure and function of Arctic ecosystems.

KEYWORDS
Arctic, F_v/F_m, kelp, laminarin, mannitol, phlorotannins, pigments, polar day, polar night, species distribution model

INTRODUCTION

Global warming is a main driver of global biodiversity loss and leads to the redistribution of species worldwide (Sunday et al., 2012; Wilson et al., 2019). Compared to the global average, Arctic regions have warmed nearly four times faster over the last four decades (Rantanen et al., 2022), with similar trends observed in air temperature and sea surface temperature (SST; Skogseth et al., 2020). The rapid temperature increase particularly threatens polar coastal ecosystems, which form an ecologically exceptional environment with a unique biological diversity (Bringloe et al., 2020).

Changes in aquatic temperature regimes directly affect physiological and biochemical processes of organisms and have been identified as a main predictor of biogeographic patterns in seaweeds (Adey & Steneck, 2001; Fragkopoulou et al., 2022; Lüning, 1990). Consequently, temperature changes have drastic effects on the distribution of marine species worldwide, especially at their warm and cold distribution margins (Sunday et al., 2012, 2015). In the Arctic, warming leads to an increase in new substrates and habitats for intertidal and subtidal species due to the associated fast sea ice melting and glacier retreats (Krause-Jensen et al., 2020). Therefore, polar areas are of special interest to ecologists, to document and understand the effects of rapid temperature changes on the redistribution of taxa (Assis et al., 2022; Bringloe et al., 2020 and Callaghan et al., 2004). Modeling studies provide an excellent approach to predict ongoing northward distributional shifts of temperate seaweeds as a result of increasing SSTs (Assis et al., 2022; Assis, Araújo, & Serrão, 2018; Krause-Jensen et al., 2020). It is assumed that the higher habitat availability in the Arctic (Krause-Jensen et al., 2020) will favor the invasion of nonpolar species, with consequences for the structure and function of Arctic communities (Wassmann et al., 2011); however, to date, we still lack knowledge about changes in seaweed abundance and their effects on the Arctic environment (Filbee-Dexter et al., 2019). Invasive seaweeds or changes in species' diversity can have extensive cascading consequences on the functioning of native ecosystems, such as biotic interactions between habitat formers and epiphytic biota (Thomsen et al., 2010). Thus, what the future brings is still "an uncertain path forward for the Arctic biome" (Bringloe et al., 2020, p. 22594).

Although temperature has progressively increased in polar environments, seasonal changes in light regimes have remained unaltered, with months-long periods of polar night, and constant light conditions during polar day. The annual cycle of photoperiods dictate large-scale periodic changes in reproductive biology and productivity, as the latter is the prerequisite for phototrophic carbon acquisition. Thus, light availability and photoperiod affect primary production and ecological processes at the very base of food webs in polar environments, including species composition and reproduction (Berge et al., 2015; Wiencke et al., 2009). In addition, SST also varies strongly over the year (see Table S1 in the Supporting Information). The fluctuating light and temperature conditions over the course of the year lead to adaptive responses in polar seaweeds, which adjust their life cycles to the specific polar conditions (Wiencke et al., 2009; Zacher et al., 2009).

The interaction of increasing temperatures under various photoperiodic light conditions has rarely been investigated (Lebrun et al., 2022; Roeber et al., 2021). Physiologically, the interplay of the light regime and temperature conditions is highly important in seaweeds. For example, high photon fluence rates during cold-temperature periods lead to damage at photosystem II (Niedzwiedz et al., 2024), since enzymatic repair mechanisms are too slow to maintain a functioning photosynthetic apparatus under high light stress (Farrugia Drakard et al., 2023).

Seaweeds have developed various physiological and biochemical mechanisms to acclimate to changes in environmental conditions (Hurd et al., 2014; Wiencke & Bischof, 2012 and references therein). However, they lack mobile life cycle stages for long-distance migration and are, hence, particularly affected by ongoing ocean warming (Reed et al., 2016; Straub et al., 2019). As sedentary organisms, seaweeds depend on limited dispersal mechanisms, such as release of planktonic spores, transport through external vectors, or long-distance drifting (Hurd et al., 2014; Tronholm et al., 2012). Kelps typically have adaptive mechanisms that are too slow for rapid changes in the environment (Vranken et al., 2021).

Kelp forests provide numerous ecosystem functions to associated organisms, such as shelter and food; they also act as carbon sinks (Teagle et al., 2017) and are of high economic value (Eger et al., 2023). Despite their capability to acclimate to changing environmental conditions, strong declines of kelp forests have been reported at their warm-edge distribution limits, mainly as a consequence of SST increases (Filbee-Dexter et al., 2020; Filbee-Dexter & Wernberg, 2018; Sorte et al., 2010). This situation has far-reaching consequences for biodiversity and ecosystem functioning (Wernberg et al., 2024). Concurrently, changed abundances of kelp species, such as *Saccharina latissima* and *Alaria esculenta*, have been observed in polar regions (Bartsch et al., 2016; Düsedau et al. in revision; Fredriksen & Kile, 2012). It has also been observed, however, that warming winters can have negative consequences for kelps' physiological traits, such as photosynthesis and biomass formation (Gordillo et al., 2022; Scheschonk et al., 2019).

The target species for this study, the kelp *Laminaria hyperborea* (Phaeophyceae, Laminariales), is an important ecosystem engineer that forms highly productive ecosystems along rocky shorelines from temperate to polar regions (northern Norway; Teagle et al., 2017; Smale, 2020; Wernberg et al., 2019). It occurs along European coasts between 40° N and 71° N, that is, from Northern Portugal to Northern Norway (Lüning, 1985), with a north-easternmost distribution at the Murman coast of the Kola Peninsula, Russia (Schoschina, 1997). As a perennial kelp, it can live up to 18 years in northern Norway (Sjøtun et al., 1993). It survives minimum temperatures of −1.5°C and maximum of 20°C (Bolton & Lüning, 1982; Lüning, 1986; tom Dieck, 1993), and it grows over the entire temperature range between 0°C and 20°C, with an optimum at 10°C–15°C (Bolton & Lüning, 1982, tom Dieck (Bartsch), 1992). *Laminaria hyperborea* generally reproduces from fall to mid-winter (Kain & Jones, 1975) and may also reproduce during darkness (Lüning, 1980). Moreover, the gametophytes survive and mature, albeit very slowly, down to a temperature of 0°C (Sjøtun & Schoschina, 2002), with the optimum being between 5°C and 17°C (Kain, 1979). It is therefore surprising that this kelp has not yet been reported from the High Arctic (see Box 1 below). Lüning (1986) indicated that long photoperiods in the High Arctic could be a limiting factor for the northern occurrence of *L. hyperborea*, as sporophytes thrive during short days and in complete darkness, and the formation of new lamina is decreasing with increasing day length and completely inhibited in summer (Bartsch et al., 2008; Lüning, 1986).

BOX 1

Gbif.org already lists an occurrence of "*Laminaria hyperborea*" for Spitsbergen as "human observation" (https://www.gbif.org/occurrence/2399478326). Individuals of "*L. hyperborea*" have also been reported from Isfjorden and Kongsfjorden (see Fredriksen et al., 2019 and references therein). However, it is important to note that *L. hyperborea* can be difficult to distinguish from *Hedophyllum nigripes* and *L. digitata* due to their similar morphological appearances (Dankworth et al., 2020; Longtin & Saunders, 2015). Both *L. digitata* and *H. nigripes* are observed widespread in the Arctic from the East (Spitsbergen) to the West (Canadian Arctic; Bartsch et al., 2016; Dankworth et al., 2020, Düsedau et al. in revision). As *L. hyperborea* may have been misidentified formerly and, so far, there is no molecular evidence of *L. hyperborea* from Svalbard, we are convinced that *L. hyperborea* has not yet spread throughout the High Arctic and that the observations from Spitsbergen are probably erroneous.

In studies on distribution changes of *Laminaria hyperborea*, the species was predicted to expand to Svalbard and further east in the White Sea until the end of the century (Assis et al., 2016; Assis, Araújo, & Serrão, 2018), with winter temperatures as the main driver for its distribution. However, experimental data are lacking, and the restricted capabilities of statistical models limit such predictions (Fragkopoulou et al., 2022). Seasonality as a critical abiotic factor has not yet been considered in the models on seaweed distribution in the Arctic.

In this study, we evaluated for the first time the effects of photoperiod × temperature interaction by simulating seasonal variations in temperatures and the polar light regime in a 3-month multifactorial experiment. Using *Laminaria hyperborea* as the case species, we investigated how the interplay of both factors affects physiological and biochemical traits. Our study was guided by the hypothesis that long photoperiods might be a limiting factor for the further northward distribution of *L. hyperborea*, following Lüning (1986). Accordingly, the extended periods of long days and the polar day in the High Arctic could limit the distribution of *L. hyperborea* in the low and subarctic regions. We then incorporated the physiological data into a geographical model to simulate the habitat suitability along the latitudinal gradient under different SST scenarios.

This study was driven by two research questions:

1. How does *Laminaria hyperborea* respond physiologically and biochemically to simulated past, present, and future SST conditions during different seasons in the High Arctic?
2. Will *Laminaria hyperborea* be able to spread throughout the High Arctic under future climatic conditions?

MATERIALS AND METHODS

Sampling and species identification

SCUBA divers collected adult sporophytes of *Laminaria hyperborea* at ~8 m depth near the Holmfjorden Research Station at Porsangerfjorden (Finnmark, Norway; 70.2° N 25.3° E) in late June 2022. The sporophytes were stored in a tank with fresh deep water throughflow (~10°C, S_A 31) for 1 week and then, due to technical problems, hung in the shade from the pier until further processing (13.7 ± 0.9°C, S_A 30.4 ± 0.8). In mid-July, non-meristematic discs (Ø 28 mm) from the central part (>10 cm above the meristem and >20 cm below the distal end) of 39 sporophytes (10–30 discs per sporophyte) were cut and transported moist, cool (<10°C), and dark to the Alfred Wegener Institute for Polar and Marine Research in Bremerhaven, Germany, where the experiment was conducted.

Due to difficulties in morphological identification for the digitate Laminariaceae (Longtin & Saunders, 2015), we screened all collected specimens genetically. For molecular identification of the individuals, subsamples of each collected sporophyte were preserved in silica gel. Genomic DNA was isolated using a plant genomic DNA extraction kit (DP305, Tiangen Biotech, China) according to the manufacturer's instructions. Species identification was conducted following the method developed by Mauger et al. (2021), which was based on amplification of a fragment of the mitochondrial COI gene (COI-5P). Briefly, two polymerase chain reactions (PCRs: PCR1 and PCR2) were conducted using a Taq Master Mix kit (Accurate Biology, China) and run on a T-gradient thermocycler (Biometra, Germany). The PCR primers and programs were as described in Mauger et al. (2021). Polymerase chain reaction products were visualized under UV light after electrophoresis on agarose gels stained with GelRed. Species were identified according to the patterns of amplified fragments in Mauger et al. (2021).

Experimental setup

For recovery, the samples were maintained in seawater at 5°C at 30–35 µmol photons $\cdot$ m^{-2} $\cdot$ s^{-1} (24:0 h light:dark, ProfiLux 3 with LED Mitras daylight 150, GHL Advanced Technology, Kaiserslautern, Germany) for a week (Figure 1). The applied photon fluence rate was based on measurements at a depth of ~7.5 m in Kongsfjorden, Svalbard (Niedzwiedz & Bischof, 2023a), since Kongsfjorden can be seen as a model ecosystem for the future of Arctic fjord systems (Bischof et al., 2019). After recovery, the samples were exposed to the photoperiod treatments (24:0 h light:dark—PolarDay, 18:6 h light:dark—LongDay, 0:24 h light:dark—PolarNight) and gradually acclimated to the temperature treatments (0°C, 5°C, and 10°C) over 4 days. The three temperature setups were based on winter (December, January, and February) and summer (June, July, and August) SSTs measured at 0–20 m in Kongsfjorden, Svalbard between 1980 and 2022 (see Table S1).

Each replicate ($n = 4$) was set up containing 20 "healthy" discs ($F_v/F_m > 0.6$, data not shown; Dring et al., 1996) from 8 to 10 individuals, evenly distributed and avoiding pseudo-replication. The experiment ran for 3 months. During the entire experiment, samples were kept in aerated 2-L clear plastic bottles in Provasoli-enriched artificial seawater (S_A 31, 1/40 PES, Provasoli, 1968; modifications: HEPES-buffer instead of Tris). The nutrient conditions of 1/40 PES (13.7 µmol NO_3^- $\cdot$ L^{-1}, 0.55 µmol PO_4^{3-} $\cdot$ L^{-1}) were based on realistic winter nutrient conditions in Kongsfjorden,

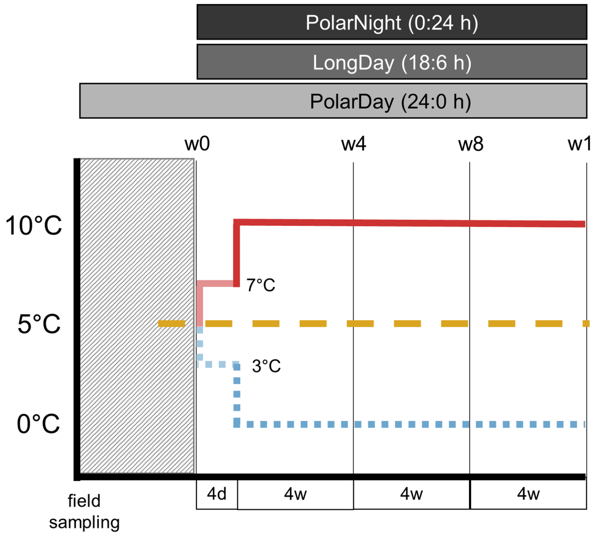

FIGURE 1 Experimental setup. Gray-dashed area: Maintenance of the field-collected sporophytes under recovery conditions in the laboratory. Week 0 (w0), w4, w8, and w12: Biochemical sampling during the experiment. Photoperiodic treatments: PolarDay = 24 h light:0 h dark, Long = 18 h light:6 h dark, PolarNight = 0 h light:24 h dark. d = days, w = week(s).

Svalbard (Norway; Bischof et al., 2019). The water was changed twice a week. Experimental sampling was conducted after 3 days of recovery (w0), in week 4 (w4), in week 8 (w8), and at the end of the experiment (w12).

Physiological parameters

The physiological vitality of all samples was checked as photosynthetic activity every week by measuring the maximum quantum yield of photosystem II (in vivo chlorophyll-fluorescence of photosystem II; F_v/F_m) using a pulse-amplitude-modulated fluorometer (Imaging-PAM, Walz GmbH, Effeltrich, Germany). The Imaging-PAM was set up to an initial fluorescence signal (F_t) between 0.15 and 0.2.

Biomass (dry weight) of the samples was monitored every 4 weeks (w0, w4, w8, and w12). For this purpose, sample discs were randomly picked and freeze-dried (Alpha 1–4 LO plus, Martin Christ Gefriertrocknungsanlagen GmbH, Osterode am Harz, Germany) before weighing (DW in g). In addition, all discs were photographed every 2 weeks with a 9 cm^2 reference grid and their area (cm^2) analyzed with ImageJ (Version 1.52a, Java 1.8.0_112, Wayne Rasband, National Institute of Health, USA).

Biochemical parameters

For the biochemical analyses, samples were shock-frozen in liquid N_2 and stored at −80°C until further processing. The samples were freeze-dried before analyses (Alpha 1–4 LO plus, Martin Christ Gefriertrocknungsanlagen GmbH, Osterode am Harz, Germany).

Mannitol and laminarin are the main carbon storage compounds in kelps. Mannitol was analyzed after Diehl et al. (2020), using the chromatographic method by Karsten et al. (1991). Laminarin was extracted from freeze-dried material with 50 mM MOPS buffer at 4°C for 5 h and measured following the method of Becker et al. (2017) and Becker and Hehemann (2018).

Pigment composition and photo-protective mechanisms, namely de-epoxidation state of the xanthophyll cycle pigments (DPS) and phlorotannins, were also monitored every 4 weeks. Absolute pigment content of chlorophyll *a* (Chl *a*), accessory pigments (Acc = Fucoxanthin + Chlorophyll *c*2 + β-Carotin), and the pool of the xanthophyll cycle pigments (VAZ = Violaxanthin + Antheraxanthin + Zeaxanthin) were determined following Diehl et al. (2021). The DPS was calculated following Colombo-Pallotta et al. (2006). The concentration of phlorotannins was measured according to Cruces et al. (2012), following the protocol in Springer et al. (2017).

Geographic projection of experimental results

We projected F_v/F_m as response variable in a mechanistic approach (Kearney & Porter, 2009). The effect sizes of photoperiod, temperature, and exposure time with and without their interaction terms on F_v/F_m were first estimated with a generalized linear model (GLM). We included weights to account for the unequal sample sizes over the course of the experiment. Inclusion of a random term for subsample-structure (i.e., aquariums as nested variable) as tested with a generalized linear mixed effect model (GLMM) was not significant and thus omitted (not shown). The best model was selected based on the Akaike information criterion (AIC). The parameter estimates for the environmental variables were then used to make projections of the algal vitality in response to temperature and photoperiodic conditions across the geographic area of interest to predict potential suitable distribution ranges of the species under current and enhanced SSTs. We chose a conservative threshold of $F_v/F_m \leq 0.3$, as continuous low F_v/F_m results in death for kelps. Thereby, our study focused on changes in habitat suitability along a latitudinal gradient from continental Europe to Svalbard, Norway.

Preparation of environmental layers

For geographic projection of the model results, we prepared raster layers for daily photoperiod (day length) conditions and daily SST with a resolution of 5 arcmin. For daily photoperiod layers, we made one raster layer for each day of the year with photoperiod in hours per pixel based on latitude with the daylength()-function from the geosphere package for R (Hijmans et al., 2022). For daily temperature, we first downloaded monthly means of SST averaged over the years 2000–2014 (corresponding to the time span covered by the widely used BioOracle v2 data set; Assis, Tyberghein, et al., 2018) from the NOAA Optimum Interpolation (OI) SST V2 data set as provided by the NOAA PSL, Boulder, Colorado, from their website at https://psl.noaa.gov (downloaded November 28, 2022; Reynolds et al., 2002). We then used a generalized additive model (GAM) to interpolate daily SST values per pixel for our projection raster layers. The period of 2000–2014 reflects the present scenario and baseline SST conditions. To simulate future warming scenarios, we used daily SST and photoperiod data for the year 2023, which was the warmest recorded year in the North Atlantic since 1979 (Copernicus, 2023), and added 1°C.

Geographic projection of F_v/F_m

We used the final model to predict how F_v/F_m of *Laminaria hyperborea* will respond to environmental conditions over a prolonged time period (1 year) in the geographic region of interest. F_v/F_m best reflected the overall observed responses of *L. hyperborea* to the experimental treatments, although it is generally a rather dynamic parameter influenced by many external and internal factors (Diehl et al., 2024; Hurd et al., 2014 and references therein). Unlike under constant laboratory conditions, SST and photoperiod change over the course of the year with the seasons. Therefore, we iteratively predicted for every consecutive day of the year how exposure to daily resolved conditions would affect the F_v/F_m. With the final adjusted model, we predicted F_v/F_m for each pixel *j* of the temperature and photoperiod layers for each day *n* of the year: $FvFm_{n,j} \sim FvFm_{n-1,j} + \beta_1 \times \mathrm{time}_{j,n} + \beta_2 \times \mathrm{temp}_{j,n} + \beta_3 \times \mathrm{photoperiod}_{j,n} + (\text{interaction terms})$, resulting in a total number of 365 prediction layers per year. For daily predictions, time was set to the constant value of 1. We further replaced the original model intercept with the F_v/F_m value from the previous day (i.e., with $FvFm_{n-1,j}$), except for $n = 1$, for which we used the original intercept of the model. This was done because the original intercept of the model represented the F_v/F_m at the start of the laboratory experiment and, therefore, was equivalent to samples in perfect condition. For a final map, we summed for each pixel the total number of days per year with a predicted F_v/F_m below the chosen threshold of 0.3.

Laminaria hyperborea reproduces (i.e., releases spores) and grows during the fall and winter season, with the earliest and latest spore releases occurring between the middle of September and the middle of April, respectively (Kain, 1971; Lüning, 1986). Therefore, starting the year with January 1st as first day and the original intercept was feasible.

Statistical analyses and software

All statistical analyses were done with R version 4.2.2 (R Core Team, 2022). The data sets of raw data as well as residuals of models were tested for normal distribution (Shapiro–Wilk test, $p > 0.05$) and homogeneity of variance (Levene's test, $p > 0.05$) and were checked visually with dot plots (Zuur et al., 2013). As the *F*-statistic is robust to a moderate deviation from the normal distribution for small sample sizes with respect to type I errors and no beneficial effects of the transformation were observed (Blanca et al., 2017), the non-normally distributed data sets were not transformed. Linear models were fit on the data sets, using the lm function and significant differences of the response variables to the interactive fixed-effects temperature (T), photoperiod (P), and sampling time (S) were assessed using a fitted linear model using analyses of variances (ANOVA; Package: stats; R Core Team, 2022). For the parameters F_v/F_m and area, repeated measures ANOVAs were applied. Pairwise comparisons were performed, using the emmeans function with Sidak correction (Package: emmeans; Lenth, 2024). The level of significance was set to $p < 0.05$. Statistical results are summarized in Table 1.

Correlations of the response parameters were tested using Spearman correlation (function: cor.test; R Core Team, 2022), after testing for normality. Data were visualized with the ggcor function (Package: GGally; Schloerke et al., 2024).

For all analyses and plotting of the species distribution model, we used R version 4.2.2 (R Core Team, 2022) with the packages terra (Hijmans, 2023), tidyr (Wickham et al., 2024), ggplot2 (Wickham, 2016), mgcv (Wood, 2023), tmap (Tennekes, 2018), and lme4 (Bates et al., 2015).

RESULTS

All statistical results are summarized in Table 1 and are not given in the plots and the text for overview reasons.

Species identification

Based on our molecular-genetic data, 37 specimens were identified as *Laminaria hyperborea* while two specimens were determined as *Laminaria digitata* (Figure S1a–c in the Supporting Information). Unfortunately, two out of 20 discs were assigned to *L. digitata* in all treatment replicates 2 and 3. These *L. digitata* discs could not be identified during the experiments and, hence, could not be excluded a priori, but with only 10% "contamination" by a wrong taxon, we are confident that the data are representative for the target species.

Physiology

The physiological vitality expressed as maximum quantum yield of photosystem II (F_v/F_m; Figure 2) of *Laminaria hyperborea* was highly affected by temperature ($p < 0.001$), photoperiod ($p < 0.001$), and their interaction (T × P; $p < 0.001$). The samples were particularly stressed when long photoperiods were paired with cold temperatures. Significant decreases in F_v/F_m were determined already after 2 weeks (w2) at 0°C under Polar Day (=0-PolarDay) and under Long Day (=0-LongDay) conditions, while vitality of samples at the 5°C Polar Day treatment (=5-PolarDay) started to diminish only in w6. After 3 months (w12), the lowest F_v/F_m values were recorded at 0-PolarDay, with values of 0.34 ± 0.07. Both a shorter photoperiod in combination with very low temperatures of 0°C and higher temperatures under PolarDay conditions resulted in significantly higher F_v/F_m values (0-LongDay: 0.53 ± 0.06; 5-PolarDay:

TABLE 1 Statistics of the physiological and biochemical parameters of *Laminaria hyperborea*.

Parameters	*p*-values	Direct comparison	
F_v/F_m			
T	**<0.001**	0°C < 5°C < 10°C	
P	**<0.001**	PD < LD < PN	
S	**<0.001**	w0 > w12	0-PD, 5-PD 0-LD
T × P	**<0.001**	Strong interaction	
DW			
T	**0.009**	0°C ≤ (5°C = 10°C)	
P	**<0.001**	PD > LD > PN	
S	**<0.001**	w0 < w12	0-PD, 5-PD, 10-PD 0-LD, 5-LD, 10-LD
T × P	**0.007**	Moderate interaction	
T × S	**0.005**		Increasing impact of T throughout the experiment
P × S	**<0.001**		Increasing impact of P throughout the experiment
T × P × S	0.335		
Chl *a*			
T	**<0.001**	(0°C = 5°C) < 10°C	
P	**<0.001**	(PD = LD) < PN	
S	**<0.001**	w0 > w12	0-PD, 5-PD, 10-PD 0-LD, 5-LD
T × P	0.057	No interaction	
T × S	**0.002**		Increasing impact of T throughout the experiment
P × S	**0.011**		Increasing impact of P throughout the experiment
T × P × S	0.135		
Acc			
T	**<0.001**	(0°C = 5°C) < 10°C	
P	**<0.001**	(PD = LD) < PN	
S	**<0.001**	w0 > w12	0-PD, 5-PD, 10-PD 0-LD, 5-LD
T × P	0.263	No interaction	
T × S	**<0.001**		Increasing impact of T throughout the experiment
P × S	**0.004**		Increasing impact of P throughout the experiment
T × P × S	0.228		
VAZ			
T	0.086	0°C = 5°C = 10°C	
P	0.305	PD = LD = PN	
S	**<0.001**	w0 > w12	0-PD, 5-PD, 10-PD 0-LD, 5-LD
T × P	0.923	No interaction	
T × S	**0.003**		Increasing impact of T throughout the experiment
P × S	**<0.001**		Increasing impact of P throughout the experiment
T × P × S	**0.029**		
DPS			
T	**<0.001**	0°C > 5°C > 10°C	w12: no sign w8: PD/LD ➔ 0°C > 5°C > 10°C PN ➔ (0°C = 5°C) > 10°C
P	**<0.001**	(PD = LD) > PN	w12: no sign w8: 0°C ➔ PD-LD (<**0.001**) 0°C ➔ PD-PN (<**0.001**) 5°C ➔ PD-PN (<**0.001**)

(Continues)

TABLE 1 (Continued)

Parameters	*p*-values	Direct comparison	
S	**<0.001**	w0 = w12	But: w0 < w8
T × P	**<0.001**	Strong interaction	
T × S	**<0.001**		Increasing impact of T throughout the experiment
P × S	**0.001**		Increasing impact of P throughout the experiment
T × P × S	**0.016**		Increasing impact of T × P throughout the experiment
Phlorotannins			
T	0.319	0°C = 5°C = 10°C	
P	0.416	PD = LD = PN	
S	0.177	w0 = w12	Exception: 0-PN (w0 < w12 **)
T × P	0.054	No interaction	
T × S	0.082		
P × S	0.661		
T × P × S	0.164		
Mannitol			
T	0.491	0°C = 5°C = 10°C	
P	**<0.001**	(PD = LD) > PN	
S	**0.006**	w0 = w12	Exception: 10-PN (w0 > w12 ***)
T × P	0.483	No interaction	
T × S	0.624		
P × S	**<0.001**		Increasing impact of P throughout the experiment
T × P × S	0.557		
Laminarin			
T	**<0.001**	0°C < (5°C = 10°C)	
P	**<0.001**	(PD = LD) > PN	
S	**<0.001**	w0 < w12	5-PD, 10-PD 5-LD
T × P	**<0.001**	Strong interaction	
T × S	**<0.001**		Increasing impact of T throughout the experiment
P × S	**<0.001**		Increasing impact of P throughout the experiment
T × P × S	0.185		

Note: Significances are highlighted in bold.

Abbreviations: Acc, accessory pigments; Chl *a*, chlorophyll *a*; DPS, de-epoxidation state of the xanthophyll cycle; T, temperature; DW, dry weight; F_v/F_m, maximum quantum yield of photosynthesis; LD, LongDay; P, photoperiod; PN, PolarNight; S, Sampling Time; PD, PolarDay; VAZ, pool of xanthophyll cycle pigments.

0.48 ± 0.05) in w12. All 10°C samples, as well as all PolarNight samples and the 5-LongDay treatment, remained above F_v/F_m values of 0.6 during the entire period, independently from the photoperiod.

Dry weight (DW in g; Figure 3) of the samples was mainly affected not only by the different photoperiods ($p < 0.001$) but also by temperature ($p < 0.01$). Although all samples weighed approximately the same at the beginning of the experiment (w0, $p > 0.05$), significant increases in DW were determined for PolarDay ($p < 0.001$) and LongDay ($p < 0.001$) over time (sampling [S]: $p < 0.001$). Further, particularly the interaction of longer photoperiods and higher temperatures resulted in the strongest weight gains with weights up to 184% ± 14% in the 10-PolarDay treatment (T × P; $p < 0.01$). Although PolarNight conditions had no significant effect on DW, a trend toward weight loss (0-PolarNight 87% ± 18%, 5-PolarNight 90% ± 10%, 10-PolarNight 93% ± 7%) was observed after 3 months of PolarNight exposure. A change of DW due to growth or shrinking of the samples can be excluded since none of the treatments revealed a significant difference in area (cm^2) between w0 and w12 (data not shown here but uploaded to the PANGAEA database; see Data Availability Statement below).

Storage carbohydrates

Although larger differences in mannitol (mg · g^{-1} DW) and laminarin (mg · g^{-1} DW) content were measured in the samples in w0, none of the treatments differed significantly regarding either carbohydrate.

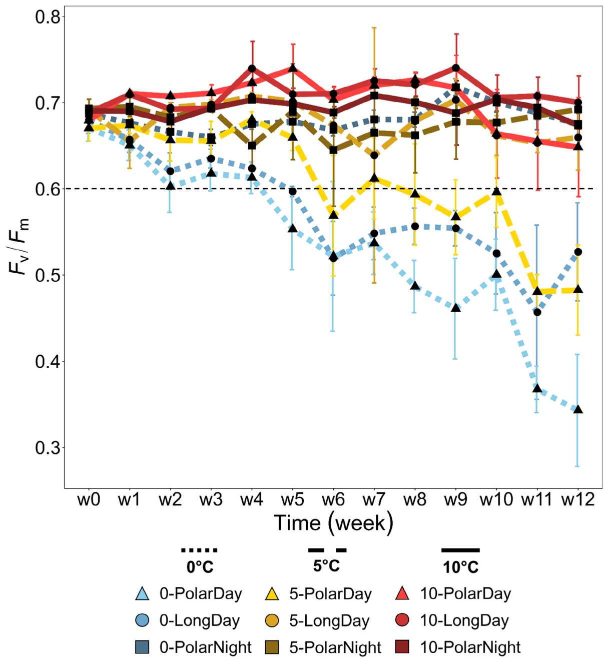

FIGURE 2 Vitality (maximum quantum yield of photosystem II; F_v/F_m) of *Laminaria hyperborea* (*L. hyperborea*), monitored weekly over 3 months under different temperature and photoperiod combinations. Values are means ± *SD* (*n* = 4). The threshold for a “good” (viable) physiological status at 0.6 is marked by the black dotted line (Dring et al., 1996).

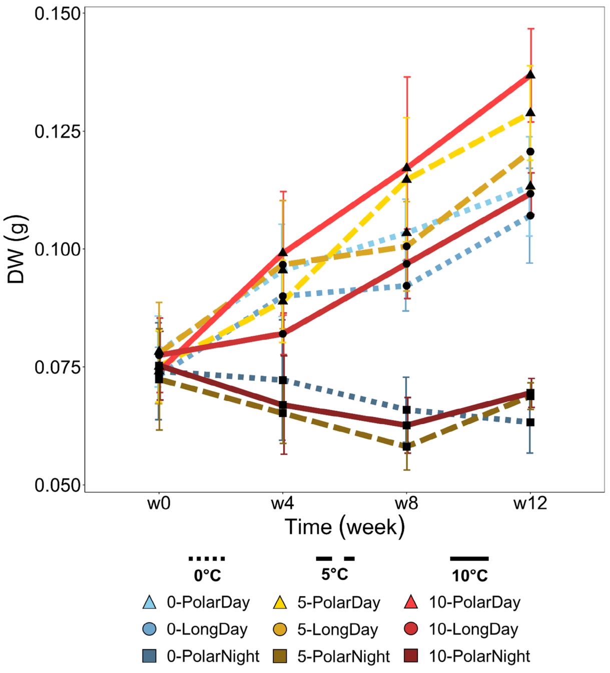

FIGURE 3 Dry weight (DW) of *L. hyperborea*, monitored every 4 weeks over 3 months under different temperature and photoperiod combinations. Values are means ± *SD* (*n* = 4).

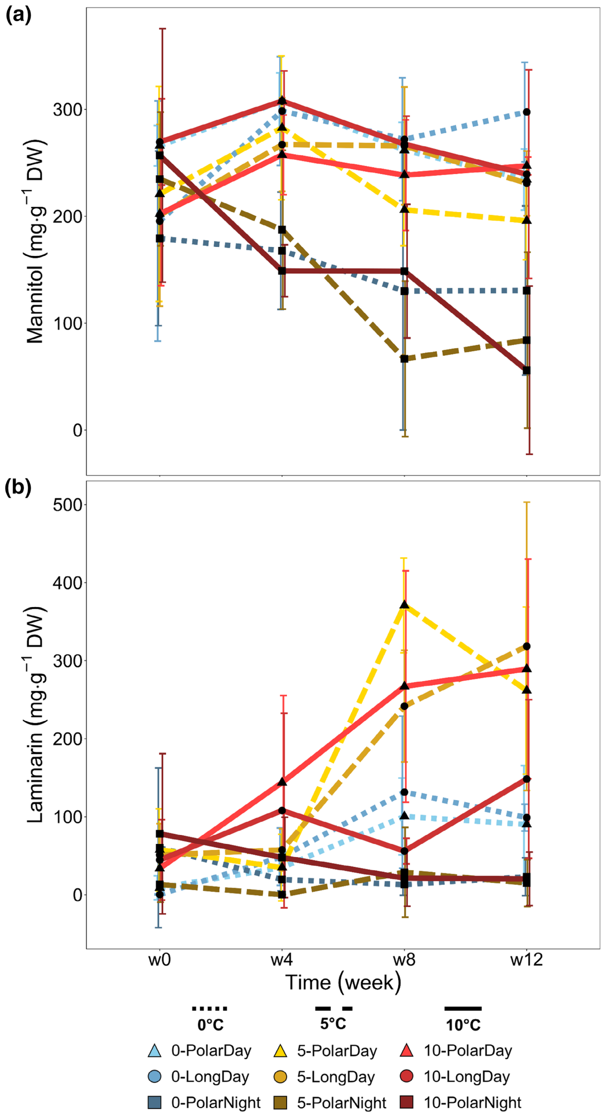

FIGURE 4 Storage carbohydrates of *L. hyperborea*, monitored every 4 weeks over 3 months under different temperature and photoperiod combinations. (a) Mannitol (b) Laminarin. Values are means ± *SD* (*n* = 4).

We did not measure significant changes in mannitol (Figure 4a) at PolarDay and LongDay, whereas the concentrations decreased at PolarNight, progressively more with increasing temperatures, while the opposite was determined for laminarin (Figure 4b). Its content remained the same for PolarNight, but increased significantly at PolarDay and LongDay.

Mannitol was strongly affected by the different photoperiods ($p < 0.001$), whereas neither temperature alone, nor T × P had a significant impact during the experiment. Concentrations in the PolarDay and LongDay treatments remained the same (S: $p > 0.05$), while a decrease of mannitol in PolarNight samples was observed over time. Although with ~–200 mg · g^{-1} DW, this decrease was only significant for 10-PolarNight ($p < 0.001$). A trend toward decreasing mannitol concentrations at 5-PolarNight was detectable (~–100 mg · g^{-1} DW). Yet, overall mannitol concentrations in the PolarDay and LongDay samples were significantly higher than in the PolarNight samples ($p < 0.001$). The significant decrease in the PolarNight treatments resulted in a strong positive correlation with DW over time (Figure 5).

For laminarin, strong impacts of photoperiod ($p < 0.001$), temperature ($p < 0.001$), and T × P ($p < 0.001$) were determined. Contrary to mannitol, laminarin concentration did not decrease in the PolarNight treatments, but increased during LongDay and PolarDay. Significant increases of ~200–250 mg · g^{-1} DW over time were only detected in treatments combining long photoperiods and enhanced temperatures (S: 5-LongDay $p < 0.001$; 5-PolarDay $p < 0.01$; 10-PolarDay; $p < 0.001$), resulting in significant lower laminarin concentration at 0°C than at 5°C ($p < 0.001$) and 10°C ($p < 0.01$). Accordingly, a very strong positive correlation between laminarin and DW was detected (Figure 5).

Light response parameters

Chlorophyll *a* (Chl *a*; µg · g^{-1} DW) and the accessory pigments (Acc; µg · g^{-1} DW; Table 2) decreased significantly over time under PolarDay conditions and at 0-LongDay and 5-LongDay ($p < 0.01$–0.001), while the concentrations in PolarNight-treated samples remained the same. Significant impacts of temperature were observed ($p < 0.001$), overall resulting in lower Chl *a* and Acc concentrations at 0°C and 5°C than at 10°C. Although 0-PolarDay and 5-PolarDay resulted in concentrations of about one third of the respective PolarNight treatments, Chl *a* and Acc of 10-PolarDay reached over half the concentrations of 10-PolarNight. Still, significant effects of T × P were not detected for Chl *a* and Acc. The pool of the xanthophyll cycle pigments (VAZ; µg · g^{-1} DW; Table 2) revealed no significant differences between the photoperiods or temperature, but also decreased exclusively in the PolarDay, 0-LongDay, and 5-LongDay treatments over time ($p < 0.05$–0.001). No significant T × P was detected. All three pigment groups revealed a strong positive correlation with F_v/F_m in the course of the experiment (Figure 5).

No significant difference of the de-epoxidation state of the xanthophyll cycle (DPS; Figure 6) was observed in any of the treatments between w0 and w12, although significant increases were determined in w8

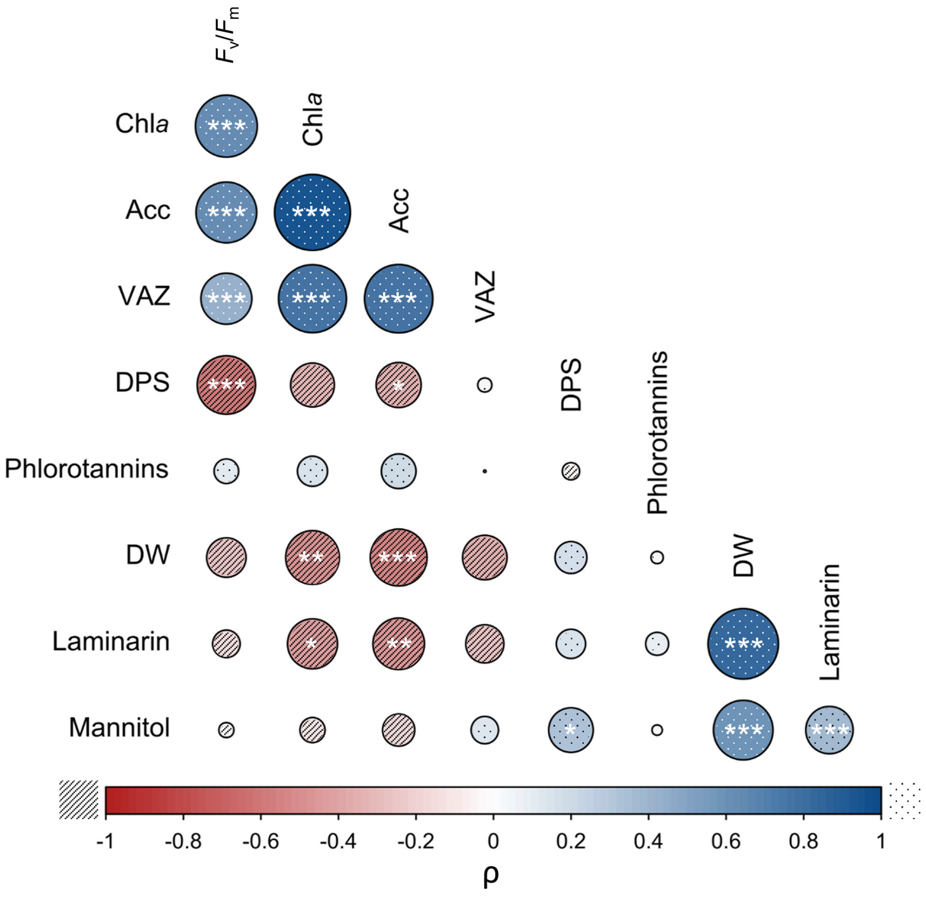

FIGURE 5 Correlation matrix of the physiological and the biochemical parameters in the course of the experiment. Acc, accessory pigments; Chl *a*, chlorophyll *a*; DPS, de-epoxidation state of the xanthophyll cycle; DW, dry weight; F_v/F_m, maximum quantum yield of photosynthesis; VAZ, pool of xanthophyll cycle pigments. The value of the correlation coefficient Spearsman's Rho (ρ) is represented by color/shading (dashed = negative correlation, dotted = positive correlation), shading and size of the circles (the darker and larger, the stronger the correlation). Significances: *$p < 0.05$, **$p < 0.01$, and ***$p < 0.001$.

TABLE 2 Biochemical light responses of *Laminaria hyperborea*, monitored every 4 weeks over 3 months (w0, w4, w8, and w12).

Parameters	Temperature (°C)	Photoperiod	w0	w4	w8	w12
Chl*a* (µg · g^{-1} DW)	0	PolarDay	1236.4 ± 90.7	610.8 ± 153.1	371.6 ± 106.4	335.4 ± 101.7
		LongDay	1286.6 ± 203.7	847.9 ± 220.2	644.4 ± 133.2	446.3 ± 62.2
		PolarNight	1206.0 ± 177.4	826.3 ± 313.9	815.1 ± 202.5	902.1 ± 146.8
	5	PolarDay	1049.6 ± 121.2	910.1 ± 76.5	519.1 ± 119.0	347.9 ± 58.0
		LongDay	1112.6 ± 172.4	672.2 ± 444.2	606.3 ± 116.1	534.6 ± 92.9
		PolarNight	1064.5 ± 194.4	955.9 ± 136.8	862.5 ± 269.7	959.4 ± 171.2
	10	PolarDay	1114.7 ± 330.2	1049.5 ± 292.7	1217.8 ± 608.1	428.3 ± 140.1
		LongDay	993.8 ± 357.7	1158.3 ± 134.4	936.4 ± 25.1	653.6 ± 89.8
		PolarNight	1186.5 ± 156.1	1024.6 ± 200.4	868.1 ± 250.2	800.4 ± 203.4
Acc (µg · g^{-1} DW)	0	PolarDay	835.6 ± 83.9	346.3 ± 89.0	287.6 ± 65.8	263.4 ± 84.5
		LongDay	819.6 ± 132.3	499.9 ± 140.9	455.7 ± 75.1	336.4 ± 47.3
		PolarNight	788.1 ± 140.0	500.5 ± 212.3	518.9 ± 114.5	646.4 ± 70.5
	5	PolarDay	661.3 ± 114.0	526.0 ± 51.8	319.2 ± 92.2	264.1 ± 56.8
		LongDay	704.1 ± 135.2	380.9 ± 252.4	385.6 ± 75.2	360.6 ± 54.9
		PolarNight	636.8 ± 133.1	536.2 ± 111.8	420.6 ± 115.5	600.6 ± 120.7
	10	PolarDay	671.8 ± 213.3	586.8 ± 181.0	632.8 ± 99.8	326.2 ± 80.4
		LongDay	580.7 ± 234.2	712.4 ± 84.0	607.5 ± 36.1	456.7 ± 58.5
		PolarNight	712.5 ± 79.8	655.3 ± 124.6	549.5 ± 177.9	538.8 ± 162.6
VAZ (µg · g^{-1} DW)	0	PolarDay	98.5 ± 33.1	41.0 ± 15.3	31.6 ± 16.7	21.9 ± 7.3
		LongDay	71.7 ± 20.6	55.7 ± 21.2	57.9 ± 14.8	26.4 ± 1.3
		PolarNight	61.3 ± 20.0	28.6 ± 14.6	50.4 ± 19.4	55.3 ± 11.5
	5	PolarDay	51.5 ± 15.0	58.0 ± 3.1	43.4 ± 12.0	21.3 ± 4.7
		LongDay	65.7 ± 16.0	34.6 ± 24.1	45.9 ± 10.7	33.5 ± 8.9
		PolarNight	42.1 ± 17.7	40.7 ± 5.7	46.6 ± 7.6	41.4 ± 6.7
	10	PolarDay	58.3 ± 20.0	61.7 ± 18.2	47.4 ± 16.0	25.1 ± 7.3
		LongDay	57.4 ± 11.2	66.6 ± 9.8	54.3 ± 5.7	38.4 ± 9.2
		PolarNight	53.2 ± 8.5	54.1 ± 13.3	42.7 ± 13.5	41.5 ± 15.0
Phlorotannins (mg · g^{-1} DW)	0	PolarDay	11.6 ± 3.1	11.4 ± 3.5	12.0 ± 7.4	10.7 ± 6.3
		LongDay	10.8 ± 6.2	12.5 ± 2.4	9.6 ± 5.0	15.3 ± 6.7
		PolarNight	11.5 ± 4.8	12.9 ± 7.3	16.5 ± 6.6	24.5 ± 11.9
	5	PolarDay	13.4 ± 2.0	7.9 ± 1.2	12.2 ± 8.5	11.6 ± 4.9
		LongDay	13.2 ± 3.0	10.0 ± 1.8	13.3 ± 5.4	12.7 ± 4.8
		PolarNight	14.8 ± 3.9	11.0 ± 4.8	7.8 ± 3.6	11.9 ± 6.4
	10	PolarDay	13.8 ± 4.5	11.6 ± 2.1	18.1 ± 7.4	16.4 ± 8.5
		LongDay	12.7 ± 6.9	12.8 ± 3.7	12.2 ± 4.8	8.0 ± 4.4
		PolarNight	19.4 ± 6.1	8.0 ± 4.2	13.1 ± 3.8	9.4 ± 5.6

Note: Values are means ± *SD* ($n = 4$).

Abbreviations: Acc, accessory pigments; Chl *a*, chlorophyll *a*; VAZ, pool of xanthophyll cycle pigments.

for 0-PolarDay ($p < 0.001$), 0-LongDay ($p < 0.001$), and 5-PolarDay ($p < 0.01$). In w8, both PolarDay and LongDay at 0°C showed significantly higher DPS than PolarNight ($p < 0.001$), while at 5°C only PolarDay differed significantly from PolarNight ($p < 0.001$). At 10°C, no differences in the photoperiod treatments were observed, highlighting the strong impact of T × P on DPS ($p < 0.001$). In the first 8 weeks of the experiment, lower temperatures in combination with longer photoperiods led to increased DPS, which, however, was compensated after 12 weeks. Nonetheless, the increased DPS resulted in a strong negative correlation of DPS and F_v/F_m in the course of the experiment (Figure 5).

Concentrations of phlorotannins (mg · g^{-1} DW, Table 2) in all treatments remained the same over the entire experiments; accordingly, they were neither affected by the treatment temperatures or photoperiods alone, nor by their interaction (T × P). No significant correlation with F_v/F_m was detected (Figure 5).

Modeling of future distribution

The best model-fit was achieved with $F_v/F_m \sim \text{time} \times \text{photoperiod} + \text{time} \times \text{temperature} \times \text{photoperiod}$. None of the variables alone had a significant effect on F_v/F_m, but the interaction terms of time × photoperiod and time × temperature × photoperiod and the intercept were highly significant with $p < 0.0001$ (β-estimate for time × photoperiod = −0.0001390, and β-estimate for time × temp × photoperiod = 0.0000193, intercept = 0.68, Table S2 in the Supporting Information).

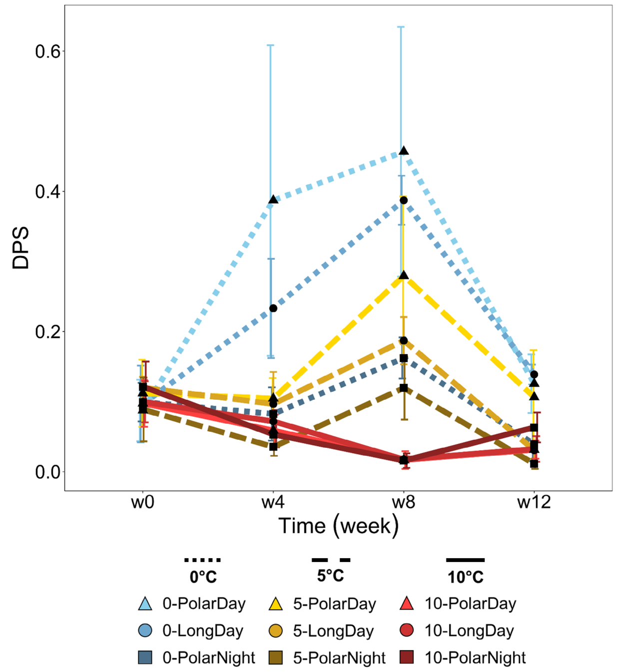

FIGURE 6 De-epoxidation state of the xanthophyll cycle pigments (DPS) of *Laminaria hyperborea*, monitored every 4 weeks over 3 months under different temperature and photoperiod combinations. Values are means ± *SD* ($n = 4$).

The geographic projections of the final model show distinctly different results for the two temperature scenarios. For scenario 1 (daily SST averaged over the years 2000–2014, Figure 7a), the area of the Spitsbergen Archipelago is predicted to exhibit environmental conditions under which F_v/F_m is expected to be ≤0.3 for over 289–337 days per year. The F_v/F_m threshold was set to 200 days below 0.3, which represents the present-day distribution limit. A continuous F_v/F_m of <0.3 would mean death for kelps. Most of the known distributional range is in areas which experience such conditions for 0 days per year, except for populations from northern Iceland and in northernmost Norway, where populations might be exposed for up to 134 and 110 days, respectively. Under scenario 2 (daily SST in 2023 + 1°C, Figure 7b), the isoclines shift northward and eastward, following increasing temperatures and indicating less adverse conditions. The isocline of 200 days with predicted $F_v/F_m \leq 0.3$ per year now reaches the western coast of the Spitsbergen Archipelago. Here, the number of days with $F_v/F_m \leq 0.3$ per year now ranges from 177 to 337 days. For Iceland, northernmost Norway, and the Russian coast, the environmental conditions are

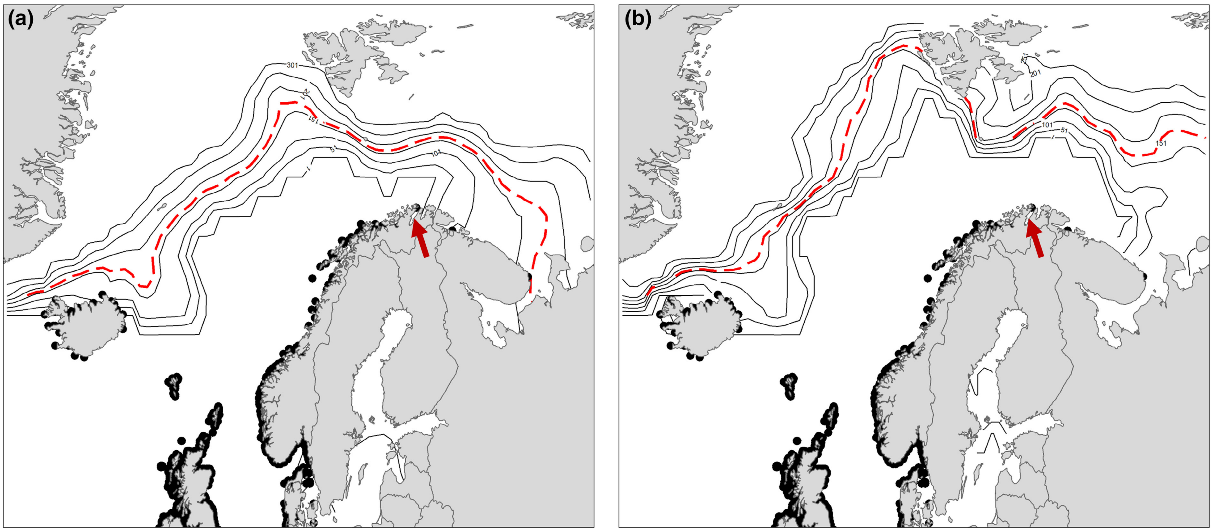

FIGURE 7 Species distribution model of *Laminaria hyperborea* modeling temperature × photoperiod interactions. Model used for predictions: $FvFm_{n,j} \sim FvFm_{j,n\text{-}1} - 0.0001390 * \text{time}_{n,j} \times \text{photoperiod}_{n,j} + 0.0000193 * \text{time}_{n,j} \times \text{temp}_{n,j} \times \text{photoperiod}_{n,j}$, with n = day of year and j = pixel. Black dots show the current distribution of *L. hyperborea* in this region as obtained from www.gbif.org excluding the record for Spitsbergen (see Introduction) (https://doi.org/10.15468/dl.jhppyr, November 2022; Mikhaylova, 2010; pers. comm. T.A. Mikhaylova). The arrows mark the sampling location at Porsangerfjorden, Norway (Finnmark). (a) Map shows sum of days per year with predicted $F_v/F_m \leq 0.3$ (survival limit for kelps), daily SST averaged over the period 2000–2014. The dotted line marks the F_v/F_m threshold of 200 days below 0.3, which represents the present-day distribution limit. (b) Map shows future prediction for sum of days per year with $F_v/F_m \leq 0.3$, daily SST for 2023 + 1°C. The dotted line is shifted under elevated SST.

predicted to cause less days of physiological stress per year.

DISCUSSION

This study emphasizes the importance of studying the combined effects of abiotic variables on seaweeds and their distribution potential. Our results clearly show that the interaction of photoperiods and temperatures had a greater influence on *Laminaria hyperborea* than either factor alone and that elevated temperatures lead to an increase in habitat suitability of High Arctic environments for *L. hyperborea*. In fact, increasing temperatures counteracted impairing photoperiodical effects. We showed that photoperiods must especially be included when it comes to predicting distributions of seaweeds and other primary producers under polar conditions.

Warming of the High Arctic—Curse or blessing for *Laminaria hyperborea*?

Although *Laminaria hyperborea* survives within the temperature ranges of the High Arctic and could, in principle, also grow and reproduce (i.e., gametogenesis, sporogenesis; Bolton & Lüning, 1982, tom Dieck (Bartsch), 1992, Sjøtun & Schoschina, 2002), the species has not yet been observed at such high latitudes (Bartsch et al., 2016, Düsedau et al. in revision). Lüning (1986) suggested that the extended periods of long days in High Arctic regions might be a limiting factor for its distribution, as day lengths of 16 h or more inhibited the formation of new fronds. However, the interactive effects of prolonged light availability with rising temperature have not been tested in the latter study. Hence, it remained uncertain whether global warming will lead to an opening of the High Arctic for *L. hyperborea*.

We observed a diminished physiological vitality ($F_v/F_m < 0.6$; Figure 2) of *Laminaria hyperborea* at longer photoperiods, ≥18 h, confirming our leading hypothesis that long photoperiods act as stressors. Additionally, the photoperiodical stress was intensified by low temperatures (0°C PolarDay: $F_v/F_m \sim 0.3$, 0°C LongDay: $F_v/F_m \sim 0.5$, 5°C PolarDay: $F_v/F_m \sim 0.5$). However, rising temperatures counteracted the impairing effects of extended day length. Temperatures of 5°C and 10°C at LongDay resulted in F_v/F_m values >0.6 reflecting "healthy" conditions (Dring et al., 1996), while at 10°C *L. hyperborea* was unaffected even under PolarDay conditions. In this context, it is important to point out that all treatment temperatures were below the species' optimum of 15°C (Bolton & Lüning, 1982).

The strong impact by the interaction of photoperiod and temperature was also observed in the monitored DW of *Laminaria hyperborea*. Samples exposed to ≥18 h of daylight significantly gained weight, with greater increases measured at ≥5°C. For the treatments, any potential effect of growth on DW can be excluded, as the discs' surface area did not change throughout the experiment. Accordingly, *L. hyperborea* must have altered and stored metabolic products causing the weight gain. Since we observed a significant increase in the long-term carbohydrate reserve laminarin at long photoperiods, which was also amplified ≥5°C, we can assume that the gain in DW was mainly caused by the additional storage of laminarin. Laminarin concentration increased strongly by ~200% when light was available, while mannitol as the primary product of photosynthesis and short-term storage carbohydrate did not rise. These results confirmed that *L. hyperborea* was still able to photosynthesize efficiently and convert mannitol to laminarin (Graiff et al., 2018; Yamaguchi et al., 1966), although it was physiologically stressed during long photoperiods.

The beneficial effects of rising temperatures during conditions of ≥18 h of daylight were also reflected in adjustments of the photosynthetic apparatus. At the end of the experiment, significantly higher concentrations of Chl *a* and Acc were detected at 10°C compared to 0°C and 5°C. Moreover, the content of Chl *a*, Acc, and VAZ decreased significantly over time during PolarDay and cold LongDay conditions. Comparable patterns with reduced Chl *a* concentration under high light conditions and increased concentrations with enhanced temperatures have also been observed for kelps from Greenland (Niedzwiedz et al., 2024). Higher plants reduce their pigment content under the combined effect of high light and low temperature to reduce excitation pressure and avoid freezing damage (Lütz, 1996). Accordingly, we assume that the reduced pigment concentrations in *Laminaria hyperborea* and other Arctic kelps at low temperatures and light stress served as a photo-protective and anti-freezing mechanism.

The photo-protective mechanism DPS significantly increased up to w8 under low temperature and long photoperiodic conditions. In contrast, at 10°C a decrease in DPS was observed. Yet, the strong disparities between the treatments weakened considerably by w12. This effect might be an indication for an acclimation of *Laminaria hyperborea* to light stress after prolonged exposure. Considering that the antioxidant phlorotannins also act as photo-protectants under prolonged PAR (photosynthetically active radiation) conditions (Steinhoff et al., 2012), it is surprising that we did not observe any response of phlorotannins to the long photoperiods. With means of 8–24 mg · g^{-1} DW, *L. hyperborea* generally contained high concentrations of phlorotannins compared to other kelps collected in the High Arctic (1 and 3.5 mg · g^{-1} DW; Diehl & Bischof, 2021; Diehl et al., 2023), which most probably already provided sufficient protection against the intense light exposure during polar day.

Under PolarNight conditions, F_v/F_m of *Laminaria hyperborea* was completely unaffected and independent of temperature. As in the case of the kelp *Saccharina latissima* (Gordillo et al., 2022), which has a similar southern distribution limit as *L. hyperborea* (Araújo et al., 2016), all samples of *L. hyperborea* remained in "healthy" conditions throughout the experiment at PolarNight ($F_v/F_m > 0.6$; Dring et al., 1996). Also regarding DW, no significant changes were observed after 3 months of total darkness in *L. hyperborea*. Contrary to other kelp species such as *Alaria esculenta*, *S. latissima*, and *L. solidungula* lost weight during long periods of total darkness and under conditions of increasing temperatures during polar night (Gordillo et al., 2022; Scheschonk et al., 2019). Throughout the long polar night in the Arctic, mannitol and laminarin in *L. solidungula* and *S. latissima* strongly decreased (Scheschonk et al., 2019), which, however, could not be confirmed for *L. hyperborea* in this study, as it kept laminarin and preferentially utilized mannitol. In contradiction to the findings by Scheschonk et al. (2019), higher temperatures at PolarNight did not result in an enhanced consumption of the storage carbohydrates. *Laminaria hyperborea* was presumably not affected by prolonged polar night conditions, as the species can be considered a "season anticipator" (Wiencke et al., 2009), as evidenced by its growth only under photoperiods <12 h (Lüning, 1986).

We did not detect any changes after 3 months of PolarNight or due to the different temperature treatments, which is in accordance with the in situ observations by Scheschonk et al. (2019) on *Laminaria solidungula* and *Saccharina latissima* before and after the polar night period in Kongsfjorden (Svalbard). The fact that we additionally observed no differences in the temperature treatments at PolarNight, could be caused by a lack of need of further protection against excitation pressure at low temperatures in total darkness (Lütz, 1996).

Past and current seasonal Arctic environmental conditions have limited, so far, the spread of *Laminaria hyperborea* sporophytes to higher latitudes (see Box 1). However, our experiment clearly indicated that higher SSTs enable this kelp also to cope with so far unfavorable photoperiods ≥18 h, while present and future polar night conditions neither impaired nor promoted *L. hyperborea*. Consequently, the physiological and biochemical results of our long-term experiment suggest a possible northward expansion of *L. hyperborea* as a result of climate change in the Arctic.

Heading northward?

Various model studies predicted a strong migration and increase in abundance for many seaweeds northward in the Arctic, including *Laminaria hyperborea* (Assis et al., 2022; Assis, Araújo, & Serrão, 2018; Frigstad et al., 2020). However, Arctic photoperiods have not been integrated in such seaweed distribution models.

Clear beneficial effects of increasing temperatures during long photoperiods on the physiological or biochemical status of *Laminaria hyperborea* were observed, and this kelp proved to be well adapted to current and future High Arctic winter conditions. The F_v/F_m data set can be treated as an integrated indicator of overall fitness and survival. Therefore, we used these data in a mechanistic species distribution model, since inclusion of physiological data can improve the predictive power of species distribution models (Kearney & Porter, 2009, Laeseke et al., 2020; Martínez et al., 2015). Our model confirmed the assumptions of the experiments: *L. hyperborea* will be able to spread into the High Arctic if SST continues to increase. When modeling the potential distribution of *L. hyperborea* under the warming scenario, the SST during the year was high enough for the species to spread throughout western Svalbard, albeit with extended photoperiods. However, for the present-day scenario (2000–2014), SST in the High Arctic was not suitable for the colonization of *L. hyperborea* on the coasts of Svalbard, as physiological performance was impaired during polar days.

Nevertheless, there are some limitations in our study that need further exploration. We cannot exclude the possibility that there are other factors limiting the northward expansion of *Laminaria hyperborea*. At low temperatures (0°C), for example, gametogenesis, germination of spores, and growth of primary cells of *L. hyperborea* were observed, but development and growth were slow (tom Dieck (Bartsch), 1992, Sjøtun & Schoschina, 2002). Sjøtun and Schoschina (2002) assumed that the strongly delayed development of gametophytes during cold winters and the high mortality risk could be the limiting factor for the spread of *L. hyperborea* in the High Arctic. The development of spores and gametophytes, as well a response of young sporophytes, must therefore be tested under the same experimental conditions to assess the viability of the different life-history stages under High Arctic conditions.

In addition, environmental conditions might further alter habitat suitability for *Laminaria hyperborea*. Sediment inputs lead to changes in underwater light climate along the Arctic coastal regions (Gattuso et al., 2020; Konik et al., 2021) and kelp canopies themselves drastically change the light availability inside kelp communities (Laeseke et al., 2019). Both effects have considerable impact not only on Arctic kelps, as they reduce incident radiation and thus weaken light stress, but also on primary production and maximum depth distribution (Laeseke et al., 2019; Niedzwiedz & Bischof, 2023b). Accordingly, it is possible that decreased light availability further reduces photoperiodic stress for *L. hyperborea* in the High Arctic, leading to a higher habitat suitability. Our model further suffers from a lack of data on recovery of *L. hyperborea* after exposure to unfavorable conditions. Thus, it remains unknown whether *L. hyperborea* can recover from long photoperiods throughout the year. Both these effects must be investigated and considered in the future.

Ecological implications

Arctic coastal ecosystems form an exceptional environment with a unique biodiversity that is under high risk due to rapid warming (Bringloe et al., 2020). Warming and consequential loss of sea ice will result in a gain of suitable habitats for intertidal and subtidal species in polar areas (Krause-Jensen et al., 2020), which, in turn, can lead to an invasion of nonpolar species and to a reorganization of species composition of ecological communities (Wassmann et al., 2011). New species or changes in species' diversity and abundance can have multiple consequences on the functioning of marine ecosystems, such as changes in the carbon cycle (Vilas et al., 2020), shifts in biotic interactions (Gilson et al., 2021), or changes in the habitat function (Christie et al., 2022; Gouraguine et al., 2024; Smale et al., 2015). *Laminaria hyperborea* is a strong competitor that displaces other kelp species, as has been observed in the Northeast Atlantic (Lüning, 1990). Contrary to other structurally similar kelps which are abundant in the High Arctic, such as *L. digitata*, the stipe of *L. hyperborea* is rich in epibiont assemblages, including Rhodophyta, Bryozoa, Polychaeta, and many more (Christie et al., 2003, 2009; Schultze et al., 1990). The epibiotic community in turn acts, for example, as food source for associated mobile species, such as fish and sea urchins (King et al., 2021; Norderhaug et al., 2005). Hence, the spread of *L. hyperborea* in the High Arctic might have cascading effects on the entire ecosystem.

AUTHOR CONTRIBUTIONS

Nora Diehl: Conceptualization (lead); data curation (equal); visualization (lead); writing – original draft (lead). **Philipp Laeseke:** Data curation (supporting); methodology (supporting); software (lead); visualization (supporting); writing – review and editing (equal). **Inka Bartsch:** Project administration (supporting); resources (lead); writing – review and editing (equal). **Margot Bligh:** Methodology (equal); writing – review and editing (equal). **Hagen Buck-Wiese:** Methodology (equal); writing – review and editing (equal). **Jan-Hendrik Hehemann:** Methodology (equal); resources (supporting); writing – review and editing (equal). **Sarina Niedzwiedz:** Data curation (supporting); methodology (equal); writing – review and editing (equal). **Niklas Plag:** Methodology (equal); writing – review and editing (equal). **Ulf Karsten:** Methodology (supporting); resources (supporting); writing – review and editing (equal). **Tifeng Shan:** Methodology (equal); writing – review and editing (equal). **Kai Bischof:** Funding acquisition (lead); project administration (lead); supervision (lead); writing – review and editing (equal).

ACKNOWLEDGMENTS

The authors are grateful to H.-K. Strand from the Holmfjorden Research Station of the Norwegian Institute for Marine Research for the support and logistics, and to the scientific diving team T. Wernberg, K. Filbee-Dexter, and T. Souster for sampling at Porsangerfjorden. N. Diehl thanks S. Jungblut and M. Koch for the support in sample preparation and M. Trautmann for weighing in the samples. The authors also thank R. Schlegel for his support in the modeling studies and the analysis of the temperature data. The experiment has been conducted at the Alfred Wegener Institute for Polar and Marine Research (AWI), Bremerhaven. The authors also thank A. Wagner (AWI) for his support in the setup of the experiment, and B. Iken (University of Bremen) for supporting the pigment analyses. Open Access funding enabled and organized by Projekt DEAL.

FUNDING INFORMATION

This study was conducted in the frame of the project FACE-IT (The Future of Arctic Coastal Ecosystems-Identifying Transitions in Fjord Systems and Adjacent Coastal Areas). FACE-IT has received funding from the European Union's Horizon 2020 research and innovation programme under grant agreement No 869154. Ulf Karsten thanks the Deutsche Forschungsgemeinschaft for funding the project “Seasonal kelp primary production at a rocky shore site: Integrating physiology and biochemistry into ecological modeling” (GR5088/2-1). [Correction added on 20 September 2024, after first online publication: In the last sentence of Funding information, “United Kingdom” was changed to “Ulf Karsten” in this version.]

DATA AVAILABILITY STATEMENT

The physiological and biochemical data analyzed for this study are uploaded on the PANGAEA Database (doi: 10.1594/PANGAEA.967510).

ORCID

Nora Diehl https://orcid.org/0000-0002-7245-340X
Philipp Laeseke https://orcid.org/0000-0003-1477-7163
Inka Bartsch https://orcid.org/0000-0001-7609-2149
Margot Bligh https://orcid.org/0000-0002-7945-7956
Hagen Buck-Wiese https://orcid.org/0000-0002-4807-5795
Jan-Hendrik Hehemann https://orcid.org/0000-0002-8700-2564
Sarina Niedzwiedz https://orcid.org/0000-0003-2604-2527
Niklas Plag https://orcid.org/0009-0009-1823-4984
Ulf Karsten https://orcid.org/0000-0002-2955-0757
Tifeng Shan https://orcid.org/0000-0003-3117-8365
Kai Bischof https://orcid.org/0000-0002-4497-1920

REFERENCES

Adey, W. H., & Steneck, R. S. (2001). Thermogeography over time creates biogeographic regions: A temperature/space/time-integrated model and an abundance-weighted test for benthic marine algae. *Journal of Phycology*, *37*, 677–698.

Araújo, R. M., Assis, J., Aguillar, R., Airoldi, L., Bárbara, I., Bartsch, I., Bekkby, T., Christie, H., Davoult, D., Derrien-Courtel, S., Fernandez, C., Fredriksen, S., Gevaert, F., Gundersen, H., le Gal, A., Lévêque, L., Mieszkowska, N., Norderhaug, K. M., Oliveira, P., … Sousa-Pinto, I. (2016). Status, trends and drivers of kelp forests in Europe: An expert assessment. *Biodiversity and Conservation*, *25*, 1319–1348.

Assis, J., Araújo, M. B., & Serrão, E. A. (2018). Projected climate changes threaten ancient refugia of kelp forests in the North Atlantic. *Global Change Biology*, *24*, e55–e66.

Assis, J., Lucas, A. V., Bárbara, I., & Serrão, E. Á. (2016). Future climate change is predicted to shift long-term persistence zones in the cold-temperate kelp *Laminaria hyperborea*. *Marine Environmental Research*, *113*, 174–182.

Assis, J., Serrão, E. A., Duarte, C. M., Fragkopoulou, E., & Krause-Jensen, D. (2022). Major expansion of marine forests in a warmer Arctic. *Frontiers in Marine Science*, *9*, 850368.

Assis, J., Tyberghein, L., Bosch, S., Verbruggen, H., Serrão, E. A., & De Clerck, O. (2018). Bio-ORACLE v2.0: Extending marine data layers for bioclimatic modelling. *Global Ecology and Biogeography*, *27*, 277–284.

Bartsch, I., Paar, M., Fredriksen, S., Schwanitz, M., Daniel, C., Hop, H., & Wiencke, C. (2016). Changes in kelp forest biomass and depth distribution in Kongsfjorden, Svalbard, between 1996–1998 and 2012–2014 reflect Arctic warming. *Polar Biology*, *39*, 2021–2036.

Bartsch, I., Wiencke, C., Bischof, K., Buchholz, C. M., Buck, B. H., Eggert, A., Feuerpfeil, P., Hanelt, D., Jacobsen, S., Karez, R., Karsten, U., Molis, M., Roleda, M. Y., Schubert, H., Schumann, R., Valentin, K., Weinberger, F., & Wiese, J. (2008). The genus *Laminaria sensu lato*: Recent insights and developments. *European Journal of Phycology*, *43*, 1–86.

Bates, D., Maechler, M., Bolker, B., & Walker, S. (2015). Fitting linear mixed-effects models using lme4. *Journal of Statistical Software*, *67*(1), 1–48. https://doi.org/10.18637/jss.v067.i

Becker, S., & Hehemann, J.-H. (2018). Laminarin quantification in microalgae with enzymes from marine microbes. *Bio-Protocol*, *8*, e2666.

Becker, S., Scheffel, A., Polz, M. F., & Hehemann, J. H. (2017). Accurate quantification of laminarin in marine organic matter with enzymes from marine microbes. *Applied and Environmental Microbiology*, *83*, 1–14.

Berge, J., Renaud, P. E., Darnis, G., Cottier, F., Last, K., Gabrielsen, T. M., Johnsen, G., Seuthe, L., Weslawski, J. M., Leu, E., Moline, M., Nahrgang, J., Søreide, J. E., Varpe, Ø., Lønne, O. J., Daase, M., & Falk-Petersen, S. (2015). In the dark: A review of ecosystem processes during the Arctic polar night. *Progress in Oceanography*, *139*, 258–271.

Bischof, K., Buschbaum, C., Fredriksen, S., Gordillo, F. J. L., Heinrich, S., Jiménez, C., Lütz, C., Molis, M., Roleda, M. Y., Schwanitz, M., & Wiencke, C. (2019). Kelps and environmental changes in Kongsfjorden: Stress perception and responses. In H. Hop & C. Wiencke (Eds.), *The ecosystem of Kongsfjorden, Svalbard. Advances in Polar Ecology* (pp. 373–422).Springer International,.

Blanca, M. J., Alarcón, R., Arnau, J., Bono, R., & Bendayan, R. (2017). Non-normal data: Is ANOVA still a valid option? *Psicothema*, *29*, 552–557.

Bolton, J. J., & Lüning, K. (1982). Optimal growth and maximal survival temperatures of Atlantic *Laminaria* species (Phaeophyta) in culture. *Marine Biology*, *66*, 89–94.

Bringloe, T. T., Verbruggen, H., & Saunders, G. W. (2020). Unique biodiversity in Arctic marine forests is shaped by diverse recolonization pathways and far northern glacial refugia. *Proceedings of the National Academy of Sciences of the United States of America*, *117*, 22590–22596.

Callaghan, T. V., Björn, L. O., Chernov, Y., Chapin, T., Christensen, T. R., Huntley, B., Ims, R. A., Johansson, M., Jolly, D., Jonasson, S., Matveyeva, N., Panikov, N., Oechel, W., Shaver, G., Elster, J., Henttonen, H., Laine, K., Taulavuori, K., Taulavuori, E., & Zöckler, C. (2004). Biodiversity, distributions and adaptations of arctic species in the context of environmental change. *Ambio*, *33*, 404–417.

Christie, H., Andersen, G. S., Tveiten, L. A., & Moy, F. E. (2022). Macrophytes as habitat for fish. *ICES Journal of Marine Science*, *79*, 435–444.

Christie, H., Jørgensen, N. M., Norderhaug, K. M., & Waage-Nielsen, E. (2003). Species distribution and habitat exploitation of fauna associated with kelp (*Laminaria hyperborea*) along the Norwegian coast. *Journal of the Marine Biological Association of the United Kingdom*, *83*, 687–699.

Christie, H., Norderhaug, K. M., & Fredriksen, S. (2009). Macrophytes as habitat for fauna. *Marine Ecology Progress Series*, *396*, 221–233.

Colombo-Pallotta, M. F., García-Mendoza, E., & Ladah, L. B. (2006). Photosynthetic performance, light absorption, and pigment composition of *Macrocystis pyrifera* (Laminariales, Phaeophyceae) blade from different depths. *Journal of Phycology*, *42*, 1225–1234.

Copernicus. (2023). Copernicus—Europe's Eyes on Earth. Available At: https://climate.copernicus.eu/

Cruces, E., Huovinen, P., & Gómez, I. (2012). Phlorotannin and antioxidant responses upon short-term exposure to UV radiation and elevated temperature in three South Pacific kelps. *Photochemistry and Photobiology*, *88*, 58–66.

Dankworth, M., Heinrich, S., Fredriksen, S., & Bartsch, I. (2020). DNA barcoding and mucilage ducts in the stipe reveal the presence of *Hedophyllum nigripes* (Laminariales, Phaeophyceae) in Kongsfjorden (Spitsbergen). *Journal of Phycology*, *56*, 1245–1254.

Diehl, N., & Bischof, K. (2021). Coping with a changing Arctic: Mechanisms of acclimation in the brown seaweed *Saccharina latissima* from Spitsbergen. *Marine Ecology Progress Series*, *657*, 43–57.

Diehl, N., Karsten, U., & Bischof, K. (2020). Impacts of combined temperature and salinity stress on the endemic Arctic brown seaweed *Laminaria solidungula* J. Agardh. *Polar Biology*, *43*, 647–656.

Diehl, N., Li, H., Scheschonk, L., Burgunter-Delamare, B., Niedzwiedz, S., Forbord, S., Sæther, M., Bischof, K., & Monteiro, C. (2024). The sugar kelp *Saccharina latissima* I: Recent advances in a changing climate. *Annals of Botany*, *133*, 183–211.

Diehl, N., Roleda, M. Y., Bartsch, I., Karsten, U., & Bischof, K. (2021). Summer heatwave impacts on the European kelp *Saccharina latissima* across its latitudinal distribution gradient. *Frontiers in Marine Science*, *8*, 695821.

Diehl, N., Steiner, N., Bischof, K., Karsten, U., & Heesch, S. (2023). Exploring intraspecific variability—Biochemical and morphological traits of the sugar kelp *Saccharina latissima* along latitudinal and salinity gradients in Europe. *Frontiers in Marine Science*, *10*, 995982.

Dring, M. J., Makarov, V., Schoschina, E., Lorenz, M., & Lüning, K. (1996). Influence of ultraviolet-radiation on chlorophyll fluorescence and growth in different life-history stages of three species of *Laminaria* (Phaeophyta). *Marine Biology*, *126*, 183–191.

Eger, A. M., Aguirre, J. D., Altamirano, M., Arafeh-Dalmau, N., Arroyo, N. L., Bauer-Civiello, A. M., Beas-Luna, R., et al. (2023). The kelp Forest challenge: A collaborative global movement to protect and restore 4 million hectares of kelp forests. *Journal of Applied Phycology*, *36*, 951–964.

Farrugia Drakard, V., Hollarsmith, J. A., & Stekoll, M. S. (2023). High-latitude kelps and future oceans: A review of multiple stressor impacts in a changing world. *Ecology and Evolution*, *13*, e10277.

Filbee-Dexter, K., & Wernberg, T. (2018). Rise of turfs: A new battlefront for globally declining kelp forests. *Bioscience*, *68*, 64–76.

Filbee-Dexter, K., Wernberg, T., Fredriksen, S., Norderhaug, K. M., & Pedersen, M. F. (2019). Arctic kelp forests: Diversity, resilience and future. *Global and Planetary Change*, *172*, 1–14.

Filbee-Dexter, K., Wernberg, T., Grace, S. P., Thormar, J., Fredriksen, S., Narvaez, C. N., Feehan, C. J., & Norderhaug, K. M. (2020). Marine heatwaves and the collapse of marginal North Atlantic kelp forests. *Scientific Reports*, *10*, 13388.

Fragkopoulou, E., Serrão, E. A., De Clerck, O., Costello, M. J., Araújo, M. B., Duarte, C. M., Krause-Jensen, D., et al. (2022). Global biodiversity patterns of marine forests of brown macroalgae. *Global Ecology and Biogeography*, *31*, 636–648.

Fredriksen, S., Karsten, U., Bartsch, I., Woelfel, J., Koblowsky, M., Schumann, R., Moy, S. R., Steneck, R. S., Wiktor, J. M., Hop, H., & Wiencke, C. (2019). Biodiversity of benthic macro- and microalgae from Svalbard with special focus on Kongsfjorden. In H. Hop & C. Wiencke (Eds.), *The ecosystem of Kongsfjorden, Svalbard, advances in polar ecology* (pp. 331–371). Springer.

Fredriksen, S., & Kile, M. R. (2012). The algal vegetation in the outer part of Isfjorden, Spitsbergen: Revisiting per Svendsen's sites 50 years later. *Polar Research*, *31*, 17538.

Frigstad, H., Gundersen, H., Andersen, G. S., Borgersen, G., Kvile, K. O., Krause-Jensen, D., Boström, C., Boström, C., Bekkby, T., d'Auriac, M. A., Ruus, A., Thormar, A., Asdal, K., & Hancke, K.. (2020). *Blue carbon—Climate adaptation, CO_2 uptake and sequestration of carbon in Nordic blue forests—results from the Nordic blue carbon project (Report No. 2020:541)*. Nordic Council of Ministers.

Gattuso, J. P., Gentili, B., Antoine, D., & Doxaran, D. (2020). Global distribution of photosynthetically available radiation on the seafloor. *Earth System Science Data*, *12*, 1697–1709.

Gilson, A. R., Smale, D. A., & O'Connor, N. (2021). Ocean warming and species range shifts affect rates of ecosystem functioning by altering consumer–resource interactions. *Ecology*, *102*, 1–12.

Gordillo, F. J. L., Carmona, R., & Jiménez, C. (2022). A warmer Arctic compromises winter survival of habitat-forming seaweeds. *Frontiers in Marine Science*, *8*, 1–18.

Gouraguine, A., Smale, D. A., Edwards, A., King, N. G., Jackson-Bué, M., Kelly, S., Earp, H. S., & Moore, P. J. (2024). Temporal and spatial drivers of the structure of macroinvertebrate assemblages associated with *Laminaria hyperborea* detritus in the northeast Atlantic. *Marine Environmental Research*, *198*, 106518.

Graiff, A., Ruth, W., & Karsten, U. (2018). Identification and quantification of laminarins in brown algae. In B. Charrier, T. Wichard, & C. R. K. Reddy (Eds.), *Protocols for macroalgae research* (1st ed., pp. 189–201). CRC Press.

Hijmans, R. (2023). terra: Spatial data analysis. R package version 1.7, https://CRAN.R-project.org/package=terra

Hijmans, R. J., Karney, C., Williams, E., & Vennes, C. (2022). geosphere: Spherical Trigonometry.

Hurd, C. L., Harrison, P. J., Bischof, K., & Lobban, C. S. (2014). *Seaweed ecology and physiology* (2nd ed.). Cambridge University Press.

Kain, J. M. (1971). Synopsis of biological data on *Laminaria hyperborea*. FAO Fish. Synopsis.

Kain, J. M. (1979). A view of the genus *Laminaria*. In M. Barnes (Ed.), *Oceanography and marine biology: An annual review* (pp. 101–161). Aberdeen University Press.

Kain, J. M., & Jones, N. S. (1975). The biology of *Laminaria hyperborea* VII. Reproduction of the sporophyte. *Journal of the Marine Biological Association of the United Kingdom*, *55*, 567–582.

Karsten, U., Thomas, D. N., Weykam, G., Daniel, C., & Kirst, G. O. (1991). A simple and rapid method for extraction and separation of low molecular weight carbohydrates from macroalgae using high-performance liquid chromatography, II. Intracellular inorganic ions and organic compounds. *Plant Physiology and Biochemistry*, *29*, 373–378.

Kearney, M., & Porter, W. (2009). Mechanistic niche modelling: Combining physiological and spatial data to predict species' ranges. *Ecology Letters*, *12*, 334–350.

King, N. G., Moore, P. J., Wilding, C., Jenkins, H. L., & Smale, D. A. (2021). Multiscale spatial variability in epibiont assemblage structure associated with stipes of kelp *Laminaria hyperborea* in the northeast Atlantic. *Marine Ecology Progress Series*, *672*, 33–44.

Konik, M., Darecki, M., Pavlov, A. K., Sagan, S., & Kowalczuk, P. (2021). Darkening of the Svalbard Fjords waters observed with satellite ocean volor imagery in 1997–2019. *Frontiers in Marine Science*, *8*, 699318.

Krause-Jensen, D., Archambault, P., Assis, J., Bartsch, I., Bischof, K., Filbee-Dexter, K., Dunton, K. H., Maximova, O., Ragnarsdóttir, S. B., Sejr, M. K., Simakova, U., Spiridonov, V., Wegeberg, S., Winding, M. H. S., & Duarte, C. M. (2020). Imprint of climate change on pan-Arctic marine vegetation. *Frontiers in Marine Science*, *7*, 617324.

Laeseke, P., Bartsch, I., & Bischof, K. (2019). Effects of kelp canopy on underwater light climate and viability of brown algal spores in Kongsfjorden (Spitsbergen). *Polar Biology*, *42*, 1511–1527.

Laeseke, P., Martínez, B., Mansilla, A., & Bischof, K. (2020). Future range dynamics of the red alga *Capreolia implexa* in native and invaded regions: Contrasting predictions from species distribution models versus physiological knowledge. *Biological Invasions*, *22*, 1339–1352.

Lebrun, A., Comeau, S., Gazeau, F., & Gattuso, J. P. (2022). Impact of climate change on Arctic macroalgal communities. *Global and Planetary Change*, *219*, 103980.

Lenth, R. (2024). emmeans: Estimated marginal means, aka least-squares means. R package version 1.10.0. https://CRAN.R-project.org/package=emmeans

Longtin, C. M., & Saunders, G. W. (2015). On the utility of mucilage ducts as a taxonomic character in *Laminaria* and *Saccharina* (Phaeophyceae)—the conundrum of *S. groenlandica*. *Phycologia*, *54*, 440–450.

Lüning, K. (1980). Critical levels of light and temperature regulating the gemtogenesis of three *Laminaria* species (Phaeophyceae). *Journal of Phycology*, *16*, 1–15.

Lüning, K. (1985). *Meeresbotanik—Verbreitung, Ökophysiologie und Nutzung der marinen Makroalgen*. Georg Thieme Verlag, Stuttgart.

Lüning, K. (1986). New frond formation in *Laminaria hyperborea* (Phaeophyta): A photoperiodic response. *British Phycological Journal*, *21*, 269–273.

Lüning, K. (1990). *Seaweeds—Their environment, biogeography, and ecophysiology*. John Wiley & Sons, Inc.

Lütz, C. (1996). Avoidance of photoinhibition and examples of photodestruction in high alpine *Eriophorum*. *Journal of Plant Physiology*, *148*, 120–128.

Martínez, B., Arenas, F., Trilla, A., Viejo, R. M., & Carreño, F. (2015). Combining physiological threshold knowledge to species distribution models is key to improving forecasts of the future niche for macroalgae. *Global Change Biology*, *21*, 1422–1433.

Mauger, S., Fouqueau, L., Avia, K., Reynes, L., Serrao, E. A., Neiva, J., & Valero, M. (2021). Development of tools to rapidly identify cryptic species and characterize their genetic diversity in different European kelp species. *Journal of Applied Phycology*, *33*, 4169–4186.

Mikhaylova, T. A. (2010). *Laminaria hyperborea* (Laminariaceae) on the Murman coast of the Barents Sea. *Botanicheskii Zhurnal*, *95*, 326–338.

Niedzwiedz, S., & Bischof, K. (2023a). *Irradiance data at different depths and sites for field sampling the Arctic fjord Kongsfjorden*. Pangaea Database.

Niedzwiedz, S., & Bischof, K. (2023b). Glacial retreat and rising temperatures are limiting the expansion of temperate kelp species in the future Arctic. *Limnology and Oceanography*, *68*, 1–15.

Niedzwiedz, S., Vonnahme, T. R., Juul-Pedersen, T., Bischof, K., & Diehl, N. (2024). Light-mediated temperature susceptibility of kelp species (*Agarum clathratum*, *Saccharina latissima*) in an Arctic summer heatwave scenario. *Cambridge Prisms: Coastal Futures*, *2*, 1–13.

Norderhaug, K. M., Christie, H., Fosså, J. H., & Fredriksen, S. (2005). Fish-macrofauna interactions in a kelp (*Laminaria hyperborea*) forest. *Journal of the Marine Biological Association of the United Kingdom*, *85*, 1279–1286.

Provasoli, L. (1968). Media and prospects for the cultivation of marine algae. In: Proceedings of the US-Japan Conference, Hakone, September 1966 (Japan Society of Plant Physiology), pp. 63–75.

R Core Team. (2022). *R: A language and environment for statistical computing*. R Foundation for Statistical Computing. https://www.R-project.org/

Rantanen, M., Karpechko, A. Y., Lipponen, A., Nordling, K., Hyvärinen, O., Ruosteenoja, K., Vihma, T., & Laaksonen, A. (2022). The Arctic has warmed nearly four times faster than the globe since 1979. *Communications Earth & Environment*, *3*, 168.

Reed, D., Washburn, L., Rassweiler, A., Miller, R., Bell, T., & Harrer, S. (2016). Extreme warming challenges sentinel status of kelp forests as indicators of climate change. *Nature Communications*, *7*, 13757.

Reynolds, R. W., Rayner, N. A., Smith, T. M., Stokes, D. C., & Wang, W. (2002). An improved in situ and satellite SST analysis for climate. *Journal of Climate*, *15*, 1609–1625.

Roeber, V. M., Bajaj, I., Rohde, M., Schmülling, T., & Cortleven, A. (2021). Light acts as a stressor and influences abiotic and biotic stress responses in plants. *Plant, Cell & Environment*, *44*, 645–664.

Scheschonk, L., Becker, S., Hehemann, J., Diehl, N., Karsten, U., & Bischof, K. (2019). Arctic kelp eco-physiology during the polar night in the face of global warming: A crucial role for laminarin. *Marine Ecology Progress Series*, *611*, 59–74.

Schloerke, B., Cook, D., Larmarange, J., Briatte, F., Marbach, M., Thoen, E., Elberg, A., & Crowley, J. (2024). GGally: Extension to 'ggplot2'. R package version 2.2.1, https://CRAN.R-project.org/package=GGally

Schoschina, E. V. (1997). On *Laminaria hyperborea* (Laminariales, Phaeophyceae) on the Murman Coast of the Barents Sea. *Sarsia*, *82*, 371–373.

Schultze, K., Janke, K., Krüß, A., & Weidemann, W. (1990). The macrofauna and macroflora associated with *Laminaria digitata* and *L. hyperborea* at the Island of Helgoland (German Bight, North Sea). *Helgoländer Wissenschaftliche Meeresuntersuchungen*, *4*, 39–51.

Sjøtun, K., Fredriksen, S., Lein, T. E., Rueness, J., & Sivertsen, K. (1993). Population studies of *Laminaria hyperborea* from its northern range of distribution in Norway. *Hydrobiologia*, *260/261*, 215–221.

Sjøtun, K., & Schoschina, E. V. (2002). Gametophytic development of *Laminaria* spp. (Laminariales, Phaeophyta) at low temperature. *Phycologia*, *41*, 147–152.

Skogseth, R., Olivier, L. L. A., Nilsen, F., Falck, E., Fraser, N., Tverberg, V., Ledang, A. B., Vader, A., Jonassen, M. O., Søreide, J., Cottier, F., Berge, J., Ivanov, B. V., & Falk-Petersen, S. (2020). Variability and decadal trends in the Isfjorden (Svalbard) ocean climate and circulation—An indicator for climate change in the European Arctic. *Progress in Oceanography*, *187*, 102394.

Smale, D. A. (2020). Impacts of ocean warming on kelp forest ecosystems. *The New Phytologist*, *225*, 1447–1454.

Smale, D. A., Wernberg, T., Yunnie, A. L. E., & Vance, T. (2015). The rise of *Laminaria ochroleuca* in the Western English Channel (UK) and comparisons with its competitor and assemblage dominant *Laminaria hyperborea*. *Marine Ecology*, *36*, 1033–1044.

Sorte, C. J. B., Fuller, A., & Bracken, M. E. S. (2010). Impacts of a simulated heat wave on composition of a marine community. *Oikos*, *119*, 1909–1918.

Springer, K., Lütz, C., Lütz-Meindl, U., Wendt, A., & Bischof, K. (2017). Hyposaline conditions affect UV susceptibility in the Arctic kelp *Alaria esculenta* (Phaeophyceae). *Phycologia*, *56*, 675–685.

Steinhoff, F. S., Graeve, M., Bartoszek, K., Bischof, K., & Wiencke, C. (2012). Phlorotannin production and lipid oxidation as a potential protective function against high photosynthetically active and UV radiation in gametophytes of *Alaria esculenta* (Alariales, Phaeophyceae). *Photochemistry and Photobiology*, *88*, 46–57.

Straub, S. C., Wernberg, T., Thomsen, M. S., Moore, P. J., Burrows, M. T., Harvey, B. P., & Smale, D. A. (2019). Resistance, extinction, and everything in between—The diverse responses of seaweeds to marine heatwaves. *Frontiers in Marine Science*, *6*, 763.

Sunday, J. M., Bates, A. E., & Dulvy, N. K. (2012). Thermal tolerance and the global redistribution of animals. *Nature Climate Change*, *2*, 686–690.

Sunday, J. M., Pecl, G. T., Frusher, S., Hobday, A. J., Hill, N., Holbrook, N. J., Edgar, G. J., Stuart-Smith, R., Barrett, N., Wernberg, T., Watson, R. A., Smale, D. A., Fulton, E. A., Slawinski, D., Feng, M., Radford, B. T., Thompson, P. A., & Bates, A. E. (2015). Species traits and climate velocity explain geographic range shifts in an ocean-warming hotspot. *Ecology Letters*, *18*, 944–953.

Teagle, H., Hawkins, S. J., Moore, P. J., & Smale, D. A. (2017). The role of kelp species as biogenic habitat formers in coastal marine ecosystems. *Journal of Experimental Marine Biology and Ecology*, *492*, 81–98.

Tennekes, M. (2018). tmap: Thematic maps in R. *Journal of Statistical Software*, *84*(6), 1–39. https://doi.org/10.18637/jss.v084.i06

Thomsen, M. S., Wernberg, T., Altieri, A., Tuya, F., Gulbransen, D., McGlathery, K. J., Holmer, M., & Silliman, B. R. (2010). Habitat cascades: The conceptual context and global relevance of facilitation cascades via habitat formation and modification. *Integrative and Comparative Biology*, *50*, 158–175.

tom Dieck (Bartsch), I. (1992). North Pacific and North Atlantic digitate *Laminaria* species (Phaeophyta): Hybridization experiments and temperature responses. *Phycologia*, *31*, 147–163.

tom Dieck, I. (1993). Temperature tolerance and survival in darkness of kelp gametophytes (Laminariales, Phaeophyta): Ecological and biogeographical implications. *Marine Ecology Progress Series*, *100*, 253–264.

Tronholm, A., Leliaert, F., Sansón, M., Afonso-Carrillo, J., Tyberghein, L., Verbruggen, H., & de Clerck, O. (2012). Contrasting geographical distributions as a result of thermal tolerance and long-distance dispersal in two allegedly widespread tropical brown algae. *PLoS ONE*, *7*, e30813.

Vilas, D., Coll, M., Pedersen, T., Corrales, X., Filbee-Dexter, K., Pedersen, M. F., Norderhaug, K. M., Fredriksen, S., Wernberg, T., & Ramírez-Llodra, E. (2020). Kelp-carbon uptake by Arctic deep-sea food webs plays a noticeable role in maintaining ecosystem structural and functional traits. *Journal of Marine Systems*, *203*, 103268.

Vranken, S., Wernberg, T., Scheben, A., Severn-Ellis, A. A., Batley, J., Bayer, P. E., Edwards, D., Wheeler, D., & Coleman, M. A. (2021). Genotype–environment mismatch of kelp forests under climate change. *Molecular Ecology*, *30*, 3730–3746.

Wassmann, P., Duarte, C. M., Agustí, S., & Sejr, M. K. (2011). Footprints of climate change in the Arctic marine ecosystem. *Global Change Biology*, *17*, 1235–1249.

Wernberg, T., Krumhansl, K., Filbee-Dexter, K., & Pedersen, M. F. (2019). Status and trends for the world's kelp forests. In J.-F. Hamel (Ed.), *World seas: An environmental evaluation: Vol. III. Ecological issues and environmental impacts* (2nd ed., pp. 57–78). Elsevier Ltd.

Wernberg, T., Thomsen, M. S., Baum, J. K., Bishop, M. J., Bruno, J. F., Coleman, M. A., Filbee-Dexter, K., Gagnon, K., He, Q., Murdiyarso, D., Rogers, K., Silliman, B. R., Smale, D. A., Starko, S., & Vanderklift, M. A. (2024). Impacts of climate change on marine foundation species. *Annual Review of Marine Science*, *16*, 247–282.

Wickham, H. (2016). *ggplot2: Elegant graphics for data analysis*. Springer-Verlag.

Wickham, H., Vaughan, D., & Girlich, M. (2024). tidyr: Tidy messy data. R package version 1.3.1, https://CRAN.R-project.org/package=tidyr

Wiencke, C., & Bischof, K. (2012). *Seaweed biology—novel insights into ecophysiology, ecology and utilization* (507). Springer.

Wiencke, C., Gómez, I., & Dunton, K. (2009). Phenology and seasonal physiological performance of polar seaweeds. *Botanica Marina*, *52*, 585–592.

Wilson, K. L., Skinner, M. A., & Lotze, H. K. (2019). Projected 21st-century distribution of canopy-forming seaweeds in the Northwest Atlantic with climate change. *Diversity and Distributions*, *25*, 582–602.

Wood, S. (2023). mgcv: Mixed GAM computation vehicle with automatic smoothness estimation. R package version 1.9.1. https://CRAN.R-project.org/package=mgcv

Yamaguchi, T., Ikawa, T., & Nisizawa, K. (1966). Incorporation of radioactive carbon from $H^{14}CO_3$- into sugar constituents by a brown alga, *Eisenia bicyclis*, during photosynthesis and its fate in the dark. *Plant & Cell Physiology*, *7*, 217–229.

Zacher, K., Rautenberger, R., Hanelt, D., Wulff, A., & Wiencke, C. (2009). The abiotic environment of polar marine benthic algae. *Botanica Marina*, *52*, 483–490.

Zuur, A. F., Hilbe, J., & Ieno, E. N. (2013). *A Beginner's guide to GLM and GLMM with R: A frequentist and Bayesian perspective for ecologists*. Highland Statistics.

SUPPORTING INFORMATION

Additional supporting information can be found online in the Supporting Information section at the end of this article.

Figure S1. For species identification of all 39 samples, the amplified fragment patterns of PCR1 and PCR2 were compared to those of Mauger et al. (2021). Thirty-seven specimens were identified as *Laminaria hyperborea* (Gunnerus) Foslie, while two specimens were identified as *Laminaria digitata* (Hudson) J.V. Lamouroux. Samples number 11–20 were part of another experiment and are therefore not included here.

Table S1. Minimum, maximum, and mean sea surface temperatures (SST) between 0 and 20 m depth measured in Kongsfjorden between 1980/1982 and 2018/2022. Data downloaded from http://choc.imev-mer.fr/shiny/dataAccess/ (for references see reference list).

Table S2. Parameter estimates (β) and corresponding *p*-values for the included variables from the final generalized linear model.

How to cite this article: Diehl, N., Laeseke, P., Bartsch, I., Bligh, M., Buck-Wiese, H., Hehemann, J.-H., Niedzwiedz, S., Plag, N., Karsten, U., Shan, T., & Bischof, K. (2024). Photoperiod and temperature interactions drive the latitudinal distribution of *Laminaria hyperborea* (Laminariales, Phaeophyceae) under climate change. *Journal of Phycology*, *00*, 1–19. https://doi.org/10.1111/jpy.13497